

Characterization of Organosolv Birch Lignins: Toward Application-Specific Lignin Production

Petter Paulsen Thoresen, Heiko Lange, Claudia Crestini, Ulrika Rova, Leonidas Matsakas,* and Paul Christakopoulos



Cite This: *ACS Omega* 2021, 6, 4374–4385



Read Online

ACCESS |



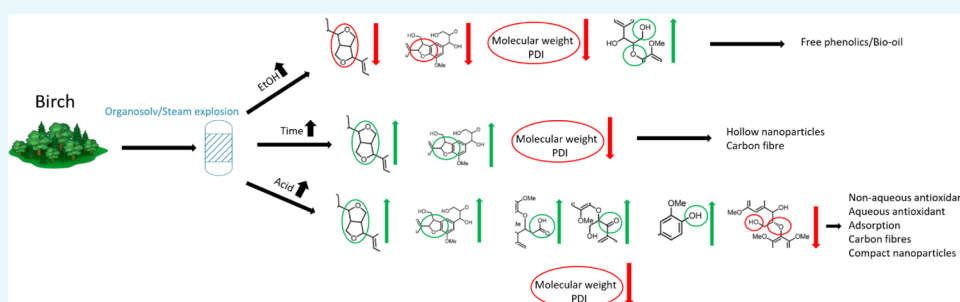
Metrics & More



Article Recommendations



Supporting Information



ABSTRACT: Organosolv pretreatment represents one of the most promising biomass valorization strategies for renewable carbon-based products; meanwhile, there is an overall lack of holistic approach to how extraction conditions affect the suitable end-usages. In this context, lignin extracted from silver birch (*Betula pendula* L.) by a novel hybrid organosolv/steam-explosion treatment at varying process conditions (EtOH %; time; catalyst %) was analyzed by quantitative NMR (^1H – ^{13}C HSQC; ^{13}C NMR; ^{31}P NMR), gel permeation chromatography, Fourier transform infrared (FT-IR), Pyr-gas chromatography–mass spectroscopy (GC/MS), and thermogravimetric analysis, and the physicochemical characteristics of the lignins were discussed regarding their potential usages. Characteristic lignin interunit bonding motifs, such as β -O-4', β - β' , and β -5', were found to dominate in the extracted lignins, with their abundance varying with treatment conditions. Low-molecular-weight lignins with fairly unaltered characteristics were generated via extraction with the highest ethanol content potentially suitable for subsequent production of free phenolics. Furthermore, β - β' and β -5' structures were predominant at higher acid catalyst contents and prolonged treatment times. Higher acid catalyst content led to oxidation and ethoxylation of side-chains, with the concomitant gradual disappearance of *p*-hydroxycinnamyl alcohol and cinnamaldehyde. This said, the increasing application of acid generated a broad set of lignin characteristics with potential applications such as antioxidants, carbon fiber, nanoparticles, and water remediation purposes.

1. INTRODUCTION

A plethora of everyday items are produced from petroleum-based compounds¹ and contribute substantially to the global economy,² but the use of nonrenewable carbon resources is also the driver behind several negative environmental impacts such as global warming and air pollution.³ An often neglected renewable component, at least when compared to the attention that sugar and syngas receives⁴ in the transition to a biomass-based society, is lignin, whose production in 2015 reached 100 million tonnes, out of which, however, only 2% were sold for applications different from energy-production through burning.⁵

The three major monomers occurring in the beforementioned polymer neglected for bio-based value-addition, namely, the lignin polymer, is *p*-coumaryl, coniferyl, and sinapyl, which upon polymerization generates the *p*-hydroxyphenyl (H), guaiacyl (G), and syringyl (S) phenylpropanoid units.⁶ In hardwoods such as birch, the overall lignin content usually amounts to 18–25%, with an S/G ratio close to 65/35.⁷ As a

result of the lignin biosynthesis occurring through radical coupling reactions, several interunit linkages occur in random sequences,⁶ the most frequent in hardwood being β -aryl-ether (β -O-4', ~80%), phenylcoumaran (β -5', 5%), resinol (β - β' , ~5%), spirodienone (β -1', 1–2%), and biphenyl ether (4-O-5', ~1%).⁷

Important to note is that the mode of extraction of lignins will affect their final chemistry as both bond cleavage and formation occur to varying extents during the process. The most common methods for lignin extraction were recently reviewed by Wang et al.,⁸ where the various extents of bond

Received: November 24, 2020

Accepted: January 19, 2021

Published: February 1, 2021



Table 1. Occurrence of Lignin Molecular Structures and molecular Weights Following the Various Treatments^a

Lignin sample	B1	B2	B3	B4	B5	B6	B7
Bonding Motif		Abundance (mmol/g) ^b					
C _α -H _α in β-O-4' structures (excl. α-OEt)	1.47	1.01	0.84	1.30	1.49	0.92	1.28
C _β -H _β in β-O-4' linked to G/H (incl. α-OEt)	0.25	0.16	0.08	0.21	0.30	0.29	0.25
C _β -H _β in β-O-4' linked to S (incl. α-OEt)	0.95	0.79	0.64	0.97	0.91	0.43	0.88
total C _β -H _β in β-O-4'	1.20	0.95	0.72	1.18	1.21	0.72	1.13
total C _α -H _α in β-O-4' (incl. α-OEt)	1.75	1.30	0.99	1.53	1.99	1.95	1.68
β-O-4' linked to S/(G + H)	3.80	4.94	8.00	4.62	3.03	1.48	3.52
oxidized (C _α) G units (aver. of C2 and C6)	0.02	0.02	0.02	0.02	0.03	0.00	0.03
oxidized (C _α) S units	0.18	0.16	0.34	0.35	0.31	0.32	0.25
C _β -H _β in α-oxidized β-O-4'	0.01	0.01	0.01	0.00	0.03	0.12	0.00
oxidized C _α S (ox. C _α /aromatic S cont.)	0.04	0.05	0.07	0.07	0.05	0.07	0.05
oxidized C _α G (ox. C _α /aromatic G cont.)	0.02	0.02	0.02	0.01	0.02	0.00	0.02
β-5' (average of C _β -H _β , C _α -H _α)	0.12	0.08	0.06	0.10	0.12	0.38	0.00
β-β' (average of C _γ -H _γ , C _β -H _β , C _α -H _α)	0.24	0.17	0.15	0.21	0.30	0.84	0.28
β-1'	0.00	0.01	0.00	0.01	0.01	0.25	0.00
C _α -ethoxylation in β-O-4' linkages	0.28	0.29	0.15	0.23	0.49	1.03	0.40
methylene OEt	1.11	0.74	0.68	0.92	2.09	9.81	2.73
methyl OEt	1.00	0.74	0.65	0.92	2.21	9.38	2.62
Lignin End Groups		Abundance (mmol/g) ^b					
p-hydroxycinnamyl alcohol (average of C _γ -H _γ , C _β -H _β , C _α -H _α)	0.05	0.02	0.01	0.02	0.08	0.00	0.00
cinnamaldehyde (average of C _β -H _β , C _α -H _α)	0.06	0.02	0.01	0.01	0.01	0.00	0.03
α methylene	0.00	0.00	0.00	0.00	0.00	0.02	0.00
Hibbert ketone, H _γ	0.00	0.00	0.00	0.00	0.04	0.28	0.00
Lignin Aromatic Units		Abundance (mmol/g) ^b					
G units (average of C ₆ and C ₂)	1.06	0.89	1.12	1.36	1.71	1.15	1.27
S units (C _{2,6} -H _{2,6})	4.01	2.95	4.27	4.90	5.85	4.34	4.79
sum S + G	5.07	3.84	5.39	6.26	7.56	5.49	6.06
ratio S/G incl. A-oxidized units	3.88	3.42	4.04	3.80	3.54	4.05	3.88
methoxy groups	7.20	5.24	4.23	6.06	9.02	11.46	8.14
Lignin Hydroxyl Group		Abundance (mmol/g) ^{c,d,f}					
aliphatic OH	3.46	3.22 ^f	3.21	3.53 ^e	3.54	1.34	2.95
C ₅ substituted/condensed OH	1.35	1.15	1.05	1.18	1.46	2.05	1.38
syringyl OH	0.40	0.33	0.35	0.34	0.40	0.74	0.44
4-O-5'	0.69	0.64	0.51	0.69	0.76	0.92	0.74
5-5'	0.21	0.18	0.14	0.13	0.24	0.35	0.17
guaiacyl OH	0.54	0.50	0.46	0.49	0.61	0.68	0.51
p-hydroxyphenyl OH	0.13	0.05	0.07	0.05	0.14	0.16	0.05
carboxylic acid OH	0.21	0.13	0.13	0.13	0.20	0.17	0.15
total phenolic OH	2.02	1.69 ^f	1.58	1.73 ^e	2.21	2.89	1.94
S-OH/G-OH	0.74	0.66	0.76	0.69	0.65	1.08	0.86
Sugar Units		Abundance (mmol/g) ^b					
β-D-xylopyranoside	0.04						
C2-H2 in β-D-xylopyranoside	0.03						
C3-H3 in β-D-xylopyranoside	0.05						
C4-H4 in β-D-xylopyranoside	0.05						
C5-H5 in β-D-xylopyranoside (overlap)							
Molecular Weight ^{e,f}							
polydispersity index (M _w /M _n)	5.8	5.6 ^f	2.7	2.7 ^e	4.9	2.0	2.7
M _w (kDa)	7.20	8.00 ^f	3.55	4.40 ^e	6.10	2.70	4.40
M _n (kDa)	1.25	1.40 ^f	1.30	1.60 ^e	1.25	1.30	1.60
Lignin Aromatic Units by Pyrolysis ^g							
S%	63	61 ^f	68	67	37	49	62
G%	34	36 ^f	30	30	60	45	34
H%	3	3 ^f	2	2	3	5	4

^aError for NMR quantification data was estimated to be ±0.1 mmol/g. ^bFrom HSQC and quantitative ¹³C NMR. ^cFrom HSQC, quantitative ³¹P NMR, and quantitative ¹³C NMR. ^dFrom GPC analysis. ^eData previously published by Mu et al.¹⁴ ^fData previously published by Muraleedharan et al.³¹ ^gFrom pyrolysis-GC/MS.

cleavage and repolymerization/condensation were summarized, and as emphasized therein, to be highly dependent on the

chosen path for lignin extraction, for example, Kraft pulping, dilute acid extraction, concentrated acid extraction, alkaline

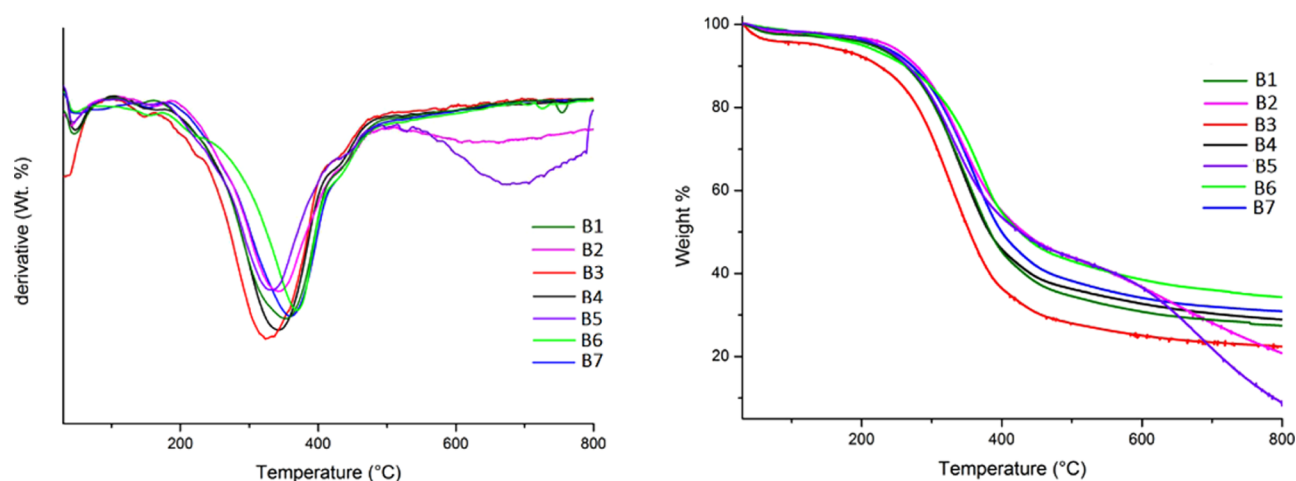


Figure 1. Derivative TGA (dTGA) and TGA curves for various treatments.

hydrolysis, ammonia-based extraction, organosolv processes, etc. As the mode of extraction heavily influences lignin chemistry, it will also influence their suitability to act as replacers for what was earlier petroleum-based constituents and thus their ability to drive the modern biorefinery toward economic viability. Among the potential high-value applications for extracted lignin, it has, for instance, been proposed as a natural, biodegradable antioxidant;^{9,10} however, its chemistry heavily dictates its radical scavenging activity.^{9,11} Other petroleum replacing applications, heavily depending on lignin chemistry, include utilization in hydrophobic composites,^{12,13} for lubricant production,^{14,15} carbon fiber production,^{16,17} nanoparticles,¹⁸ adsorption purposes in aqueous remediation systems,^{19,20} or production of low-molecular-weight aromatics and hydrocarbons.^{21,22} Despite the fact that lignin chemistry will heavily influence its suitability for a specific application, there is nowadays still a lot of need for strictly connecting isolation process parameters to chemical features of the extracted lignin and the abundance of specific structural motifs and the resulting consequences for suitable high-value applications. The current work thus sets out to investigate the application of a promising mode of extraction, namely, the novel organosolv/steam-explosion method,²³ which combines the benefits of a catalytically active solvent allowing the dissolution of hydrolyzed lignin with the shear force of depressurization made more effective by solvent-softening of cell–cell adhesion.²⁴ While the characterization of birch lignin extracted under a certain organosolv condition has been reported,²⁵ there are no reports on how changing important process parameters employed during birch processing through a combined, novel organosolv/steam-explosion mode affect the chemistry of the extracted lignins. This chemistry of the extracted lignins will be discussed with respect to the suitability of the various lignins for specific, high-value, down-stream applications.

2. RESULTS AND DISCUSSION

2.1. Characterization of Lignin Samples. ¹H–¹³C Heteronuclear single quantum coherence spectroscopy (HSQC) analysis revealed the most important structural characteristics of lignins originating from the various treatments (Table 1). Characteristic cross-peaks were quantified on the basis of quantitative ¹³C NMR analyses (Table S1: Assigned shifts. Table S2: Associated concentrations). For

quantitative HSQC analysis, the concentrations of C₂-H₂ in G units and C_α-H_α in β-O-4' structures were used to correlate the quantitative ¹³C NMR and ¹H–¹³C HSQC spectra (Figures S3–S9 for lignin B1–B7) with aromatic and aliphatic signals, respectively (for assigned shifts and structure evaluation, see Tables S3 and S4, respectively).²⁶ The results alongside those obtained for phenolic end groups and aliphatic OH groups by quantitative ³¹P NMR analyses are summarized in Table 1. To delineate whether the changes in functional group contents can be traced back to depolymerization events, molecular mass data were generated by gel permeation chromatography (GPC) and are listed together with NMR data in Table 1. The characteristic shifts associated with the monomeric units (S, G, and H) occurring in hardwoods⁷ were readily determined with an S/G ratio (3.42–4.05)²⁷ and H unit content (0.00–0.07 mmol/g)²⁶ which is in the reported range of birch and hardwoods. Also, Pyr-gas chromatography–mass spectroscopy (GC/MS) was applied to evaluate the contents of S, G, and H units (Table 1). Interestingly, these data are indicative of higher sensitivity toward the type and contents of interunit linkages. Accordingly, the S/G values for B4, B2, and B7 were 2.23, 1.69, and 1.82 by Pyr-GC/MS, whereas they amounted to 3.80, 3.42, and 3.88 by HSQC, respectively. This discrepancy can be explained by differences in the two methods, where the first requires thermal decomposition and will be affected by the thermal stability of the certain lignin motifs, while the second does not. High temperatures²⁸ and high heating rates²⁹ are required to thermally cleave and volatilize condensed structures, as opposed to structures with numerous β-O-4' linkages.³⁰ Upon lower carbon–carbon interunit linkage content, similar trends are seen.

2.2. Thermogravimetric Analysis (TGA) Analysis. The results obtained from TGA is presented in Figure 1. Apart from what seems to be an initial loss of bound water around 120 °C,³² and volatilization of residual hemicelluloses around 200 °C,²³ two major mass-loss events occur at intermediate temperatures (250–400 °C) and high temperatures (600–800 °C) from what, when seen in the light of the results presented in Table 1, seems to be due to differences in lignin chemistry and will be discussed in the sections that follow.

Apart from what is mentioned above, four events stood out.

- (1) As can be observed from Table 1 and will be further discussed in the sections covering the specific parameter effects, only the B3 treatment generated a homogenous,

- low-molecular-weight extract with intact aryl ether structures devoid of any condensation or side-chain modification. Now, considering the dTGA and TGA curves (Figure 1), such characteristics offer highly heat-labile structures.
- (2) High contents of β -O-4' linkages have been correlated to significant weight loss around 250–350 °C;³⁰ in the present work, this presented itself through the dTGA of **B4** and **B5** where the greater maxima for the former is indicative of a faster mass loss. Also, indicative of this is the similarity in thermal stability for **B2** and **B5**, while the slight maxima shift toward higher temperatures for **B2** potentially originates from its lower β -O-4' content and higher M_w . The effect from M_w is also indicated for **B2** and **B6**, where the β -O-4' content is similar. A similar balancing act between the molecular weight and β -O-4' content was seen in the dTGA curves of **B4** and **B1**, where a higher M_w seems to offer higher thermal stability despite its higher content of labile aryl ether linkages. However, while the thermal decomposition occurs faster (dTGA) for lower molecular weight lignins, the overall mass loss is greater for **B1** lignins with higher β -O-4' content in the 250–350 °C range. Noteworthy, the lower maximum of **B1** and its peak position being skewed toward higher temperatures is likely to be aided by the higher content of β - β' ³³ and β -5' structures.³⁴
 - (3) Considering the events occurring in the high-temperature region (600–800 °C), the mass loss has usually been ascribed to the degradation of aromatics and C–C bonds.³² Meanwhile, increased thermal stability of lignin linkages such as β - β' , as opposed to β -O-4',³³ could reduce initial degradation-based volatilization of further heat-labile structures until temperatures are reached that favor char formation through radical driven reactions and thus generating a greater char yield.³⁵ In light of this, **B2** and **B5** presented low stability above 500 °C despite having contents of β - β' and β -5' similar to those lignins stable in this region. However, these lignins presented the lowest dTGA maxima at 200–500 °C, despite a β -O-4' content comparable to that of lignins exhibiting greater weight losses in this temperature region. Thus, it appears that the introduction of C–C bonds (such as β - β' and β -5') can reduce the thermal degradation of structures liable such as β -O-4' at intermediate temperatures (200–500 °C) so that these instead occur in the high-temperature region (above 500 °C).
 - (4) In relation to the effect of the acidic catalyst on thermal stability, progressive addition of the catalyst seems to gradually increase the overall resistance toward thermal decomposition despite the formation of low-molecular-weight lignins (**B6**). As mentioned under point (3), this seems to originate from the introduction of C–C linkages, which compensate for the effects of less thermally stable structures like β -O-4'. Interestingly, upon the highest acid concentration (**B6**) where depolymerization has proceeded (as indicated through low M_w and M_n), the highest contents of β - β' and β -5' structures seem to yield lignins with the overall highest thermal stability. Apart from the introduction of the aliphatic condensation structures already mentioned, β -1' was also identified in **B6** (Table 1), potentially contributing to the enhanced thermal stability. Though being harder to accurately determine (vide infra, Effect

of acid concentration), there are indications that additional aliphatic condensation and eventually ethoxylation in the α -position of β -O-4' motifs occur, which may affect the thermal stability of especially the lignins extracted in the presence of acid. No significant contribution seems to originate from aromatic condensation structures as there were no changes in the ratio of quaternary carbons/tertiary carbons (from Table S2) to the overall aromatic content (S2,6 + G2; Table S4) when the acid content was increased from 0 to 1 wt %. No signals from dibenzodioxocin, biphenyl ether, or spirodienones were identified, and stilbenes were practically absent (Table S4).

2.3. Effect of Ethanol. Lignin **B1**, extracted with 50% (w/w) ethanol, is characterized by the dominating presence of β -O-4' units, presence of aliphatic condensate structures such as β - β' and β -5' and cinnamic end groups. The total aromatics content (S2,6 + G2) was 5.07 mmol/g, with a total phenol content of 2.02 mmol/g. The mean average molecular weight was 1.25 kDa, and molecular weight distribution exhibited a polydispersity index (PDI) of 5.8. As mentioned in Section S6.1, a high PDI can make for efficient energy absorption in lubricants, and if accompanied by other hydrogen bond donating/accepting components, a high overall OH group is expected to be beneficial. Indeed, **B1** lignin presents the overall highest combined aromatic and aliphatic OH-group content (5.48 mmol/g) considering the lignins evaluated in the present work, raising its potential as a component for lubrication purposes.

Furthermore, lignin **B1** presented xylan shifts in the HSQC spectra, which hint at the presence of carbohydrate residues in the sample, albeit at low concentration. These signals were absent in the other samples, suggesting that more severe conditions, including higher ethanol concentration, prolonged treatment times, and/or acid catalyst, were necessary for efficient separation of sugars. Interestingly, none of the samples displayed cross-peaks typically attributed to lignin carbohydrate complexes, suggesting that even the mildest isolation conditions, such as lowest ethanol concentration and absence of acid, were sufficient to effectively cleave any potentially present chemical links (lignin carbohydrate complexes³⁶) between the polymers.³⁷ Hence, **B1** coextraction is likely a consequence of the inefficient chemical separation of polymers.

Treatment with the highest ethanol content enabled the extraction of lignin **B3**, characterized by a low molecular weight comparable to that of **B1** but a lower PDI (2.7). The low molecular weight, lower abundances of β -O-4' structures (according to signals for C_{α} , C_{β} , and C_{γ}), continued presence of the cinnamic end-group (albeit lower), tendency toward a lower content of condensed aliphatic β - β' and β -5' structures, and a higher total content of S2,6 + G2 aromatics with more S than G in combination with a reduced total phenol content suggest oligomeric lignin exhibiting intact, i.e., nonoxidized/condensed aliphatic bonding motifs connecting more condensed/oxidized aromatic structures. This suggestion is further supported by a relatively elevated aliphatic OH-group content interpretable as a sign for the absence of side-chain condensations in light of "missing" sugar impurities. When evaluating such unaltered structural characteristics for potential applications, the production of free phenolics/bio-oil (Section S6.2) seems to suit, and while the C_{α} (β -O-4' structures) signal was relatively low, the decreased signals and content

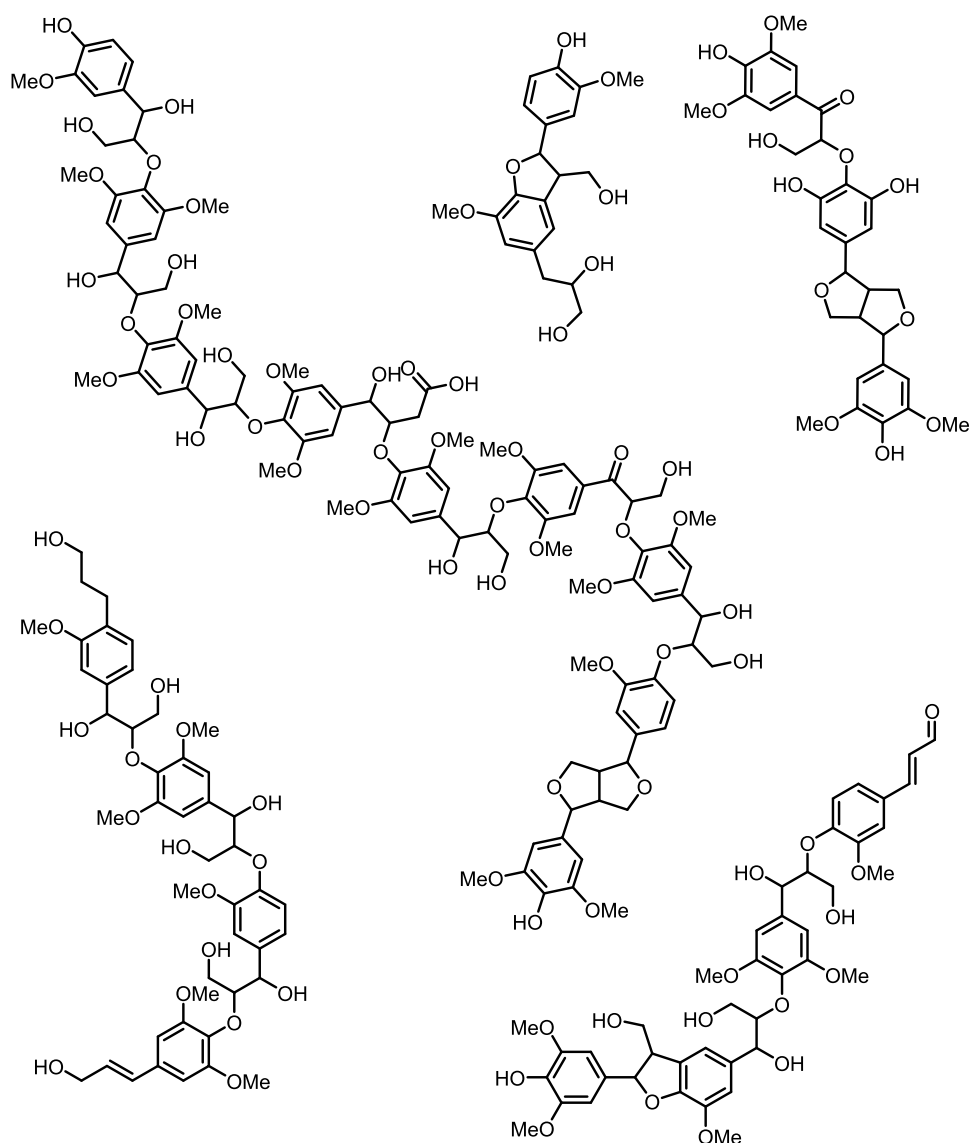


Figure 2. Examples of oligomeric organosolv birch lignin molecules obtained using extraction conditions **B1**, **B2**, and **B3**.

corresponding to C_γ , β - β' , and β -5' structures were more prominent, indicating low side-chain modification and introduction of C–C bonds. Together with low phenolic OH, M_n , M_w , and PDI, as well as the presence of *p*-hydroxycinnamyl and cinnamaldehyde end groups, this lignin is scarcely affected by the extraction process and could undergo further depolymerization. Exemplary potential structures representing **B1** and **B3** are illustrated in **Figure 2**.

2.4. Effect of Acid Concentration. Increasing process severity by the addition of acid or prolonged treatment time is often associated with the lower recovery of labile β -O-4' linkages, on the one hand, and a relative increase in more condensed structures on the other.³⁸ Changes in intramolecular bonding as a function of process parameters are also evident in the present work. The increasing acid content is found to lead to eventually fewer β -O-4' units, while the relative amount of β - β' and β -5' structure augments. This is accompanied by an increase in phenolic hydroxyls, as delineated by ³¹P NMR analysis. The aliphatic hydroxyl content eventually decreases. A significant reduction in M_w and M_n , a loss in cinnamyl aldehyde, and *p*-hydroxycinnamyl

alcohol are observed alongside a decrease in the total aromatic monomer content (S2,6 + G2). Interestingly, upon the intermediate acid content (**B5**), the content of end groups increases alongside the aromatic unit (S + G) and the β -O-4' content, suggesting efficient extraction without extensive lignin modification. However, upon the highest acid content, the β -O-4' content drastically decreases, while the data simultaneously suggest an increase in the oxidized β -O-4' structures and eventually an onset of ethoxylation of the benzylic position; abundances of β -5' and β - β' structures increase as well. The practical loss of cinnamic-type end groups found at highest acid concentrations can be interpreted as their participation in side-chain condensation reactions, which would resemble polymerization events. The latter could also contribute to an overall reduction in the standard aromatic signal that is observed, caused by the loss of aromatic C–H used for quantification or to changes in the immediate vicinity of the C2 carbon. Increasing the content of methoxy groups going from **B4**, i.e., no acid, via **B5** to **B6**, i.e., the highest acid content, can further be seen as a hint of an increased condensation, but with the absence of any notable change in

the ratio of quaternary to tertiary carbon atoms in the aromatic region (Table S2) interestingly failing to easily support the theory of any widespread condensation reactions directly involving the aromatics. The development of the methoxy group content is thus better explained by taking into consideration the nature of the biomass used in the process. G-lignin is extracted at earlier stages during organosolv treatment, whereas S-lignin gradually builds up and can be extracted only upon prolonged treatment³⁹ or acid addition to enhance delignification during treatment,¹¹ whereby in the latter case, regions naturally rich in G-lignin such as the middle lamella were readily delignified due to simultaneous fiber separation.⁴⁰ As indicated above and in Table 1, the increased acid concentration seems to gradually decrease the contents of intact β -O-4' structures (C_a) via cleavage, from 1.30 to 1.49 and 0.92 mmol/g in **B4**, **B5**, and **B6**, respectively, and this drop can eventually also be associated with an increased content S-type aromatics in the extracted lignin molecules: the loss in β -O-4' originates mostly from S-based structures such as C_β in syringyl β -O-4', which went from 0.97 (**B4**) to 0.91 (**B5**) and 0.43 mmol/g (**B6**), when comparing guaiacyl β -O-4', which augmented from 0.21 (**B4**) to 0.30 (**B5**) and 0.29 mmol/g (**B6**) according to the ¹³C NMR-based quantification of HSQC data. The increasing trends found for the S/G monomer ratio, going from **B4** to **B5** and **B6** (3.80, 3.54, 4.05, respectively), and the S-OH/G-OH ratio (0.69, 0.65, 1.08, respectively) suggest that more phenolic S units were extracted during the progressive cleavage of their β -O-4' linkages, which were found to gradually decrease (intact β -O-4' S/(G + H) ratio 4.62, 3.03, and 1.48 mmol/g for **B4**, to **B5** and **B6**, respectively). Upon introduction of the acidic catalyst in the traditional ethanol organosolv system, the formation of an intermediate α -carbocation was postulated in ethanol-based organosolv processes, allowing the ethanol to act as a nucleophile and cause ethoxylation in the α -position.⁴¹ In the present work, this structural modification was especially prominent, eventually detectable upon increasing the concentration of the acid catalyst (Table 1). Ethoxylation was also eventually observed for the longest treatment time (**B7**) but to a significantly lesser extent. It has been reported that G-lignins are more prone to ethoxylation compared to S-lignins,⁴² due to both acid extraction through enhanced dissolution in the organic phase containing the respective alcohol and the stability difference of the β -O-4' motif.⁴³ This is evident in the present work where the progressive addition of the acidic catalyst causes detectable ethoxylation and decreased aliphatic OH content, while the ratio of S-linked β -O-4' motifs (including ethoxylated β -O-4' motifs) to G-linked counterparts decreases (4.62, 3.03, 1.48; **B4**, **B5**, **B6**) in front of an overall increase of the S/G ratio (3.49, 3.59, 3.88; **B4**, **B5**, **B6**).

Apart from partial ethoxylation upon elevated catalyst content, the shifts associated with β - β' and β -5' structures eventually increase, while the aliphatic hydroxyl contents decrease due to oxidation, mentioned partial ethoxylation of the benzylic position of the β -O-4' structure, and formation of β - β' and β -5' structures. It has been further suggested that the degradation of structures such as β - β' and β -5', originally formed through aliphatic condensation, could generate aliphatic structures and new primary alcohols with different structures compared to the secondary alcohols traditionally attributed unaltered lignins, which overlaps with the signal usually associated with C_γ -H $_\gamma$ in the β -O-4' structure.⁴⁴ Such reactions cannot be fully excluded in the present work in the

case of the addition of the acid catalyst, based on elevated C_γ -H $_\gamma$ signal intensities observed, especially for **B6** (Table S4). Ethylation can also occur at residual sugar hydroxyls.⁴⁵ To check this, signals corresponding to ethoxylated anomeric carbons were evaluated.⁴⁶ While the methyl group of the ethoxylated xylose anomeric carbon overlaps with the region associated with the C_γ -H $_\gamma$ signal, a signal with shift 3.47/18.43 δ_H/δ_C could be detected for the treatment employing the highest acid content (**B6**), potentially originating from the ethylation of the said component. No methyl signal from potentially ethylated glucose⁴⁷ could be detected, though. While the signals associated with the xylose carbons are negligible for the **B6** treatment, their acid-catalyzed degradation products, including ethoxylated aliphatic structures, could contribute to the C_γ -H $_\gamma$ signal.⁴⁸ Another effect occurring in the side-chain upon the addition of acid is oxidation. Oxidation is known to affect the chemical nature of lignin upon organosolv treatment,⁴⁹ and could potentially be associated with dehydration reactions occurring during depolymerization and repolymerization events.⁵⁰ Such effects could partially explain the observed reduction in aliphatic hydroxyl groups that is observed in quantitative ³¹P NMR upon increased treatment severity, i.e., in **B6** lignin. Methylene groups (mmol/g) are observed by quantitative ¹³C NMR when transitioning from **B4** (1.10) to **B5** (1.22) and **B6** (1.42) (Table S2 and Figure S1). Additional evidence came from the appearance of an HSQC shift corresponding to α methylene at the highest acid concentration. Interestingly, as the acid concentration increased, ketones became more abundant, from 0.04 to 0.28 mmol/g in **B5**, and **B6**, respectively, as did the signal for C_β -H $_\beta$ in α -oxidized β -O-4' (0.03–0.12 mmol/g). Considering the simultaneous decrease of aliphatic hydroxyls for the mentioned treatments (3.54–1.34 mmol/g), this suggests an increasing extent of aryl ether cleavage, side-chain dehydration, and oxidation, which is reported to occur upon acidic treatments of lignins in organic media.⁵¹ Interestingly, however, for the bespoke treatments, an increase in enol ethers, stilbene, or cinnamyl contents is not observed. The onset of degradation upon severity increases via acid addition is also monitored by changes in molecular weight. **B6** lignin displays lower molecular weights alongside significantly lower PDI, suggesting substantial chemical alterations toward a rather homogenous oligomeric material.

Now, considering the effect of acid on the suitability of the extracted lignins for specific applications, several possibilities introduce themselves. For antioxidant applications, both **B5** and **B6** present high contents of aromatic OH groups and also widespread side-chain hydration, partial ethoxylation of β -aryl ethers, and condensed content. As discussed in Section S6.3, **B6** lignins would appear more suitable as antioxidants in an organic media due to their high content of aromatic OH groups, increase in β - β' and β -5' structures, few aliphatic OH groups, and the introduction of nonpolar ethyl groups. In contrast, the presence or abundance of Hibbert ketones and similar oxidized species (oxidized S units) may be detrimental. On the other hand, application in an aqueous environment would potentially suit **B5** lignins, which present high aromatic OH (2.21 mmol/g, respectively) and aliphatic OH group content (3.53 mmol/g) together with a total content of 0.03 mmol/g oxidized aryl ethers (α -oxidized β -O-4') and a low degree of ethoxylation. The precise effect of CH₃/CH₂ from the various amounts of β - β' + β -5' structures, their derivatives, and other structures is, however, difficult to predict at this

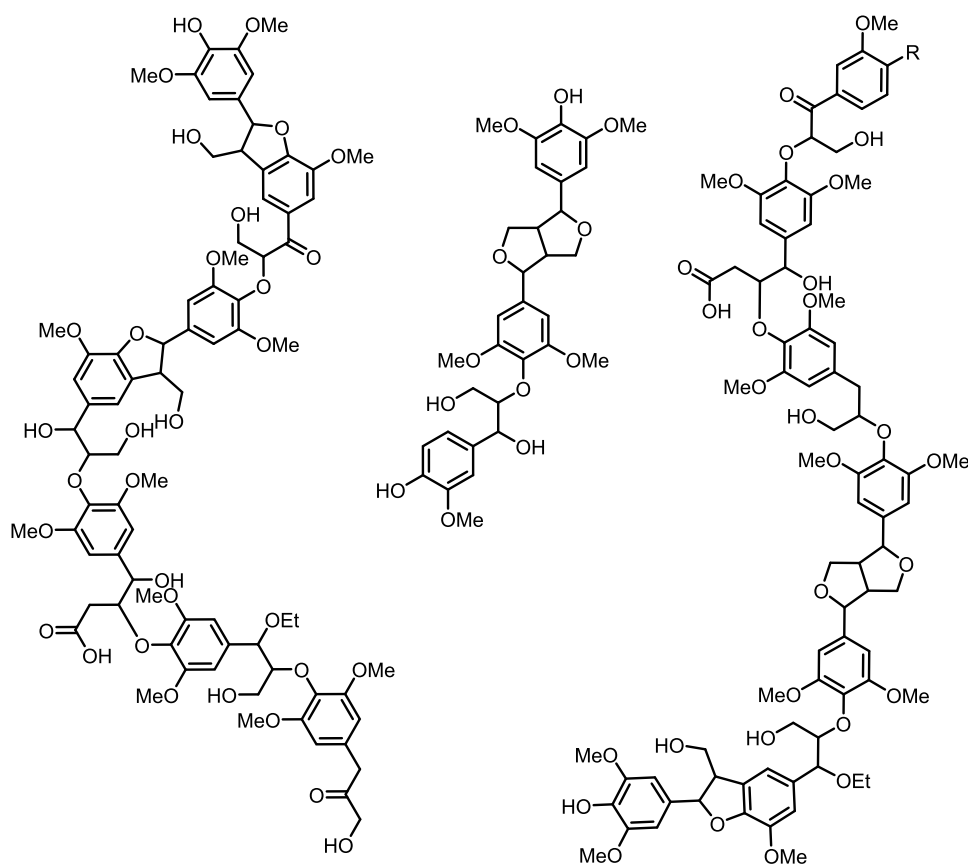


Figure 3. Examples of oligomeric organosolv birch lignin molecules obtained using extraction conditions involving acid catalyst in combination with ethanol.

point. As a second potential application encountered through the effect of adjusting the catalyst content is for adsorption purposes (Section S6.4). Again, considering the **B6** lignin, its high content of aromatics (S2,6 + G2, mmol/g), high content of aromatic OH (2.89 mmol/g), high content of oxidized S units (0.32 mmol/g), high content of Hibbert ketones (0.28 mmol/g), and numerous structures in the side-chain (C_{α} , β - β' , β -5') makes it potentially applicable for adsorption purposes. Furthermore, the low molecular weight of the **B6** lignin alongside its high thermal stability (Figure 1) could make it suitable for the production of crystalline carbon fibers (Section S6.6), while the broader PDI and lower thermal stability (Figure 1) of **B5** could allow for a more irregular structure with a larger pore size and available surface area if conductive properties are sought after. As a final potential application of the lignins originating from the variable acid content is the production of nanoparticles (Section S6.7). While both hollow and compact nanoparticles can be formed depending on the desired application, the latter seems achievable when considering the **B5** lignin due to its high PDI (4.9), high phenolic OH content (2.21 mmol/g), and high S + G phenolic content (7.56 mmol/g).

Figure 3 summarizes the consequences of acid addition on the lignin structure as observed in this study.

2.5. Effect of Time. Degradation of traditional lignin structures was reported previously when isolated organosolv lignins were re-exposed to the acidic conditions they had been originally extracted from.³⁸ This explicit observation underlines how treatment time is a crucial factor affecting the structural characteristics of lignin. Here, this is supported by comparing

the structural data of **B4**, **B2**, and **B7** lignins. Prolonged treatment times lead to a decrease in cinnamic end groups and aliphatic hydroxyls, which is largely attributable to a decrease in β -5' and the corresponding increase in β - β' structures, indicating as such an onset of internal condensations. Interestingly, however, β -O-4' linkage contents are not found to alter over time, indicating that their stability is affected mostly by acidic conditions. Nevertheless, an increased S/G content and lower molecular weights of lignins are observed as the effect of prolonged process times. This finding suggests that the reduced delignification (Table 3) derived from redeposition of large lignin structures onto gradually exposed hydrophobic cellulose surfaces, with the entropic driving force for redeposition being directly related to lignin chain length/surface area,⁵² is not only contrasted by acid addition (Table 1), which likely caused sufficient lignin depolymerization, but also by an increase of time that leads to significant and sufficient changes in the structure to facilitate the extraction of lignin, and more specifically of S-type motifs. Now, when evaluating the potential applications of the lignins extracted by adjusting the treatment time, fewer obvious routes seem to present themselves, at least when comparing to that occurring when adjusting the catalyst content. The **B7** lignin, however, presents among the lowest PDI's found in the present work (2.7), alongside relatively high contents of aliphatic and aromatic OH, as well as aromatic contents. Such chemical characteristics could be suitable when considering the formation of hollow nanoparticles (Section S6.7), where stabilization of nonideal mixing of solvents is crucial. **B6** and **B4** present chemical characteristics, which could make it

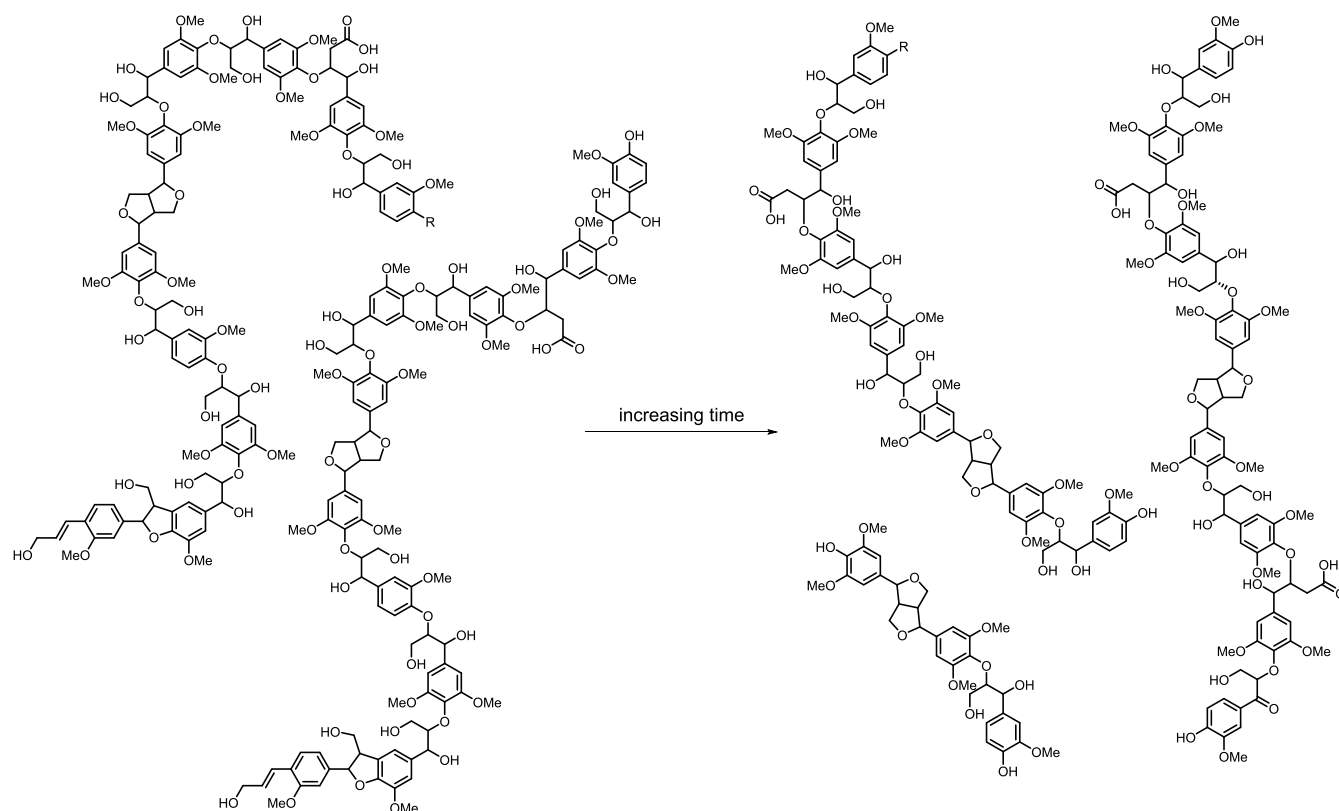


Figure 4. Examples of smaller oligomeric organosolv birch lignin molecules obtained upon increased treatment times from larger oligomeric starting structures.

suitable for carbon fiber production (Section S6.6): overall high S + G content, low PDI, alongside what seems to be relatively intact aliphatic side-chain structures acting as volatiles for structure adjustment and/or formation of porous structures.

Structural modifications eventually occurring upon prolonged reaction time are presented in Figure 4.

A summary of the possible applications, structural characteristics of lignins rendering them potentially suitable for such end uses, and the most promising treatments for greener alternatives to fossil-based chemicals is presented in Table 2.

3. CONCLUSIONS

Varying treatment conditions during the extraction of lignins by hybrid steam explosion/organosolv processing generate lignins with a wide range of structural and chemical properties. The increasing acid content continuously decreases the amount (mmol/g) of intact β -O-4' structures, especially those associated with syringyl units as opposed to guaiacyl units whose aryl ether linkages experience stabilization partially eventually also from ethoxylation. In general, however, the addition of acid gradually introduces more aliphatic condensed structures (primary condensation structures such as β - β' + β -5' and yet unidentified derived secondary structures). Simultaneously, as the aliphatic hydroxyl content decreases, more oxidized structures (C_{α} and Hibbert ketone) are introduced, traditional lignin end groups (*p*-hydroxycinnamyl alcohol and cinnamaldehyde) are removed, and the overall lignin molecular weight steadily decreases. A similar although less pronounced trend is seen upon increased treatment time, potentially due to the comparable, but weaker, mode of action presented by water. Short, nonacidic treatments yield high-molecular-weight

lignin with an elevated content of intact β -O-4' structures. Unaltered lignins with low PDI and low-molecular weights are obtained following treatment with 70% v/v ethanol. The different chemical characteristics of the isolated lignins are likely to affect their suitability for subsequent, high-value applications. Understanding the correlation between lignin isolation method/conditions, their chemical nature, and performance of the extracts for certain end-uses will determine the economic viability of lignocellulosic biorefineries.

4. MATERIAL AND METHODS

4.1. Materials. Birch lignin (Figure S2) was obtained as described by Matsakas et al.²³ In short, debarked, knife-milled (<1 mm sized) wood chips from silver birch (*Betula pendula* L.) were used as feedstocks for organosolv/steam-explosion treatment. The specific treatment conditions are listed in Table 3 alongside the achieved delignifications.

After the treatment, the slurry was vacuum-filtered to separate the solids from the liquor. Rotary evaporation reduced lignin solubility through ethanol removal. Finally, lignin was isolated by centrifugation (14 000 rpm/29 416g, at 4 °C for 15 min) before being air-dried to constant weight. All chemical reagents were of analytical grade.

4.2. Lignin Characterization. **4.2.1. Pyrolysis–Gas Chromatography–Mass Spectroscopy (Pyr-GC/MS).** Pyr-GC/MS was carried out on a Shimadzu PY-3030S pyrolyzer (pyrolysis was carried out at 550 °C) coupled to a Shimadzu GCMS-QP2010 Ultra chromatograph equipped with a Restek RTX-1701 column (60 m × 0.25 mm, id 0.25 μ m film thickness) and a quadrupole mass spectrometer detector (EI at 70 eV, ion source 240 °C). A split ratio of 1:100 and injection temperature of 280 °C were used. The temperature in the

Table 2. Chemical Characteristics of Certain Lignins and their Potential Applications

application	potential lignin characteristic	potential lignin
aqueous antioxidant	high aromatic OH content oxygen-rich (ketone or -OH) side-chain low CH ₃ /CH ₂ content in side-chain	B5
nonaqueous antioxidant	high aromatic OH content oxygen-poor (ketone or -OH) side-chain high CH ₃ /CH ₂ content in side-chain	B6
adsorbent in the aqueous environment (biochar)	high porosity and surface area (high content of potential volatiles in original lignin; intact, noncondensed propanoid side-chain and residual sugars) high oxygen (high S/G) and hydroxyl content (depolymerization) low degree of carbonization low molecular weight	B6
filler in hydrophobic composite/rubber (biochar)	low oxygen content compatible for filler–matrix interaction (electronic interactions between aromatic rings due to graphitization or increased sp ² /sp ³) compatible for filler–filler interaction (electronic interactions between aromatic rings due to graphitization or increased sp ² /sp ³)	B5
component in lubricant	high PDI or sufficient interaction between lubricant components (sufficient hydrogen bond formation)	B1
carbon fiber (high conductivity application such as electrodes or supercapacitors)	high degree of graphitization (high sp ² /sp ³) high porosity and surface area (high content of potential volatiles in original lignin; intact, noncondensed propanoid side-chain and/or residual sugars) low content of oxygen (removed during pyrolysis)	B4
carbon fiber (mechanical)	low/intermediate molecular weight with sufficient thermal mobility to ensure generation of a crystalline structure after fiber formation broader PDI to facilitate a more irregular graphitic structure with greater fiber diameter and surface area	B6
free phenolics/bio-oil	high content of β-O-4' linkages or at least low content of condensed structures	B3
compact lignin nanoparticles	presence of high-molecular-weight lignins acting as nucleation sites primarily aggregating through hydrophobic interactions	B5
hollow lignin nanoparticles	presence of amphiphilic low-molecular-weight lignins acting as stabilizers at the interphase between aqueous-organic solvents not mixing ideally	B7

Table 3. Organosolv Treatment Conditions Tested in this Study, along with their Codes and the Obtained Delignifications^{23a}

code	ethanol [% v/v]	duration [min]	H ₂ SO ₄ [% w/w biomass]	delignification [%]
B1	50	30	0.0	81.2
B2	60	30	0.0	80.5
B3	70	30	0.0	72.6
B4	60	15	0.0	77.0
B5	60	15	0.2	78.2
B6	60	15	1.0	86.2
B7	60	60	0.0	57.5

^aThe temperature and solid/liquid ratio applied for the extraction were 200 °C and 100g/L, respectively. Delignification was calculated as a fraction of Klason lignin extracted from the original material.

chromatograph oven was initially held at 40 °C for 1 min, then ramped at 8 °C/min to 270 °C, and held there for 40.25 min. Helium at a flow rate of 2.5 mL/min was used as the carrier gas. Mass spectra in the molecular mass range $m/z = 33-500$ were obtained.

4.2.2. Gel Permeation Chromatography (GPC). Molecular weight distributions of the extracted lignins were determined by GPC with a PerkinElmer Flexar high-performance liquid chromatography apparatus equipped with a Waters Styragel HR 4E column and a UV detector (absorption measured at 280 nm). During analysis, the column was kept at 40 °C and tetrahydrofuran at a flow rate of 0.6 mL/min was used as the mobile phase. Polystyrene was used for standard curve

calibration. Prior to GPC analysis, the lignins were acetobrominated as described previously.⁵³ Molecular masses calculated based on the calibration were rounded to the full hundreds.

4.2.3. Nuclear Magnetic Resonance (NMR). **4.2.3.1. Quantitative ³¹P NMR Analysis.** The hydroxyl content of isolated lignins was analyzed by quantitative ³¹P NMR with a Bruker Ascend Aeon WB 400 NMR spectrometer as previously described.¹⁴ Briefly, 120 mg of lignin was dissolved in 1.6 mL of anhydrous CDCl₃/pyridine (1:1.6 v/v) solution. Subsequently, 400 μL of anhydrous CDCl₃/pyridine containing 0.1 M cholesterol (internal standard) and 5 mg/mL Cr(III) acetylacetonate (relaxation agent) were added and the solution was mixed until it reached homogeneity. Then, 400 μL of phosphitylating reagent (2-chloro-4,4,5,5-tetramethyl-1,2,3-dioxaphospholane) was added and the solution was stirred for 2 h at room temperature before being transferred to a 10 mm NMR tube. The ³¹P NMR signal was obtained using the standard Bruker zgig sequence for 72 scans at 25 °C. The data were processed using Bruker TopSpin 3.5pl2 and quantitative analysis was performed as described before.⁵⁴

4.2.3.2. Quantitative ¹³C NMR Analysis. Lignin samples of ~80 mg were dissolved in 550 μL of DMSO-*d*₆, and 50 μL of Cr(III) acetylacetonate in DMSO-*d*₆ (~1.5 mg/mL) were added as a spin-relaxation agent, and 50 μL of trioxane (92.92 ppm) in DMSO-*d*₆ (~15 mg/mL) was used as an internal standard. Spectra were recorded at room temperature on a Bruker AVANCE 400 MHz spectrometer equipped with a 5 mm double resonance broadband inverse probe. An inverse-

gated proton decoupling pulse sequence was applied with a 90° pulse width, a relaxation delay of 1.7 s, and an acquisition time of 1.2 s. A total of 20 000–24 000 scans were acquired for each spectrum. NMR data were processed using MestreNova Version 9.0.1 (Mestrelab Research S.L.).

4.2.3.3. ^1H – ^{13}C Heteronuclear Single Quantum Coherence (HSQC) Analysis. Lignin samples of ~80 mg were dissolved in 500 μL of $\text{DMSO-}d_6$, and Cr(III) acetylacetonate was added as a spin-relaxation agent at a final concentration of ~1.5 mg/mL. HSQC spectra were recorded at 30 °C on a Bruker 400 MHz spectrometer controlled via TopSpin 3.5pl2 and equipped with a 5 mm double resonance broadband inverse probe. The Bruker hsqcetgpsisp2.2 pulse program in the DQD acquisition mode was used, with NS = 64; TD = 2048 (F2) and 512 (F1); SW = 12.9869 ppm (F2) and 164.9996 ppm (F1); O2 (F2) = 2601.36 Hz and O1 (F1) = 7799.05 Hz; D1 = 2 s; CNST2 $^1\text{J}(\text{C-H})$ = 145; and acquisition time F2 channel = 197.0176 ms and F1 channel = 15.4164 ms. The pulse length of the 90° P1 high-power pulse was optimized for each sample. NMR data were processed with MestreNova.

4.2.4. Fourier Transform Infrared (FT-IR) Analysis. A total of 1–2 mg of samples was mixed with 300 mg of KBr and prepared as disks. The spectra were recorded using a Bruker IFS 80v vacuum FT-IR spectrometer equipped with a deuterated triglycine sulfate detector using the double-side forward–backward acquisition mode under vacuum at room temperature (~22 °C). In total, 128 scans were signal-averaged and co-added at an optical resolution of 4 cm^{-1} .

4.2.5. Thermogravimetric Analysis (TGA). Briefly, 1–2 mg of various lignin samples was placed on PerkinElmer ceramic pans and subjected to TGA at 30–800 °C with a heating rate of 10 °C/min under a N_2 atmosphere using a PerkinElmer 8000 TGA apparatus.

■ ASSOCIATED CONTENT

SI Supporting Information

The Supporting Information is available free of charge at <https://pubs.acs.org/doi/10.1021/acsomega.0c05719>.

Experimental and reported NMR shifts and spectra, their structural assignments and associated concentrations; FT-IR data and peak assignments; lignin visual representation; and background and discussion on high-value lignin applications (PDF)

■ AUTHOR INFORMATION

Corresponding Author

Leonidas Matsakas – Biochemical Process Engineering, Division of Chemical Engineering, Department of Civil, Environmental and Natural Resources Engineering, Luleå University of Technology, SE-971-87 Luleå, Sweden; orcid.org/0000-0002-3687-6173; Phone: +46 (0) 920 493043; Email: leonidas.matsakas@ltu.se

Authors

Petter Paulsen Thoresen – Biochemical Process Engineering, Division of Chemical Engineering, Department of Civil, Environmental and Natural Resources Engineering, Luleå University of Technology, SE-971-87 Luleå, Sweden
Heiko Lange – Department of Pharmacy, University of Naples'Federico II', 80131 Naples, Italy

Claudia Crestini – Department of Molecular Science and Nanosystems, University of Venice Ca' Foscari, 30170 Venice Mestre, Italy; orcid.org/0000-0001-9903-2675

Ulrika Rova – Biochemical Process Engineering, Division of Chemical Engineering, Department of Civil, Environmental and Natural Resources Engineering, Luleå University of Technology, SE-971-87 Luleå, Sweden

Paul Christakopoulos – Biochemical Process Engineering, Division of Chemical Engineering, Department of Civil, Environmental and Natural Resources Engineering, Luleå University of Technology, SE-971-87 Luleå, Sweden; orcid.org/0000-0003-0079-5950

Complete contact information is available at: <https://pubs.acs.org/doi/10.1021/acsomega.0c05719>

Funding

This work was funded by the Swedish Research Council for Environment, Agricultural Sciences and Spatial Planning (Formas) under grant no 2016-20022.

Notes

The authors declare no competing financial interest.

■ ACKNOWLEDGMENTS

P.P.T., U.R., L.M., and P.C. would like to acknowledge Bio4Energy, a strategic research environment provided by the Swedish government, for supporting this work. The contribution of COST Action LignoCOST (CA17128), supported by COST (European Cooperation in Science and Technology), in promoting interaction, exchange of knowledge, and collaborations in the field of lignin valorization is gratefully acknowledged. H.L. acknowledges the MIUR Grant "Dipartimento di Eccellenza 2018–2022" to the Department of Pharmacy of the University of Naples "Federico II". C.C. acknowledges the Ca'Foscari FPI 2019 funding. We would also like to thank Dr. Shubhankar Bhattacharyya (Chemistry of Interfaces, Luleå University of Technology) for his assistance during part of the analysis of lignins.

■ REFERENCES

- (1) Lentini, J. J.; Dolan, J. A.; Cherry, C. The Petroleum-Laced Background. *J. Forensic Sci.* **2000**, *45*, No. 14819J.
- (2) Bergholt, D.; Larsen, V. H.; Seneca, M. Business Cycles in an Oil Economy. *J. Int. Money Finance* **2019**, *96*, 283–303.
- (3) Martins, F.; Felgueiras, C.; Smitkova, M.; Caetano, N. Analysis of Fossil Fuel Energy Consumption and Environmental Impacts in European Countries. *Energies* **2019**, No. 964.
- (4) Wery, T.; Petersen, G. *Top Value Added Chemicals from Biomass: Volume I—Results of Screening for Potential Candidates from Sugars and Synthesis Gas* (No. DOE/GO-102004-1992); National Renewable Energy Lab.: Golden, CO, 2004.
- (5) Bajwa, D. S.; Pourhashem, G.; Ullah, A. H.; Bajwa, S. G. A Concise Review of Current Lignin Production, Applications, Products and Their Environment Impact. *Ind. Crops Prod.* **2019**, *139*, No. 111526.
- (6) Boerjan, W.; Ralph, J.; Baucher, M. Lignin Biosynthesis. *Annu. Rev. Plant Biol.* **2003**, *54*, 519–546.
- (7) Ralph, J.; Lapierre, C.; Boerjan, W. Lignin Structure and Its Engineering. *Curr. Opin. Biotechnol.* **2019**, 240–249.
- (8) Wang, H.; Pu, Y.; Ragauskas, A.; Yang, B. From Lignin to Valuable Products—Strategies, Challenges, and Prospects. *Bioresour. Technol.* **2019**, *271*, 449–461.
- (9) Ponomarenko, J.; Dizhbite, T.; Lauberts, M.; Volperts, A.; Dobeles, G.; Telysheva, G. Analytical Pyrolysis - A Tool for Revealing

of Lignin Structure-Antioxidant Activity Relationship. *J. Anal. Appl. Pyrolysis* **2015**, *113*, 360–369.

(10) Dizhbite, T.; Telysheva, G.; Jurkane, V.; Viesturs, U. Characterization of the Radical Scavenging Activity of Lignins - Natural Antioxidants. *Bioresour. Technol.* **2004**, *95*, 309–317.

(11) Ponomarenko, J.; Dizhbite, T.; Lauberts, M.; Viksna, A.; Dobeles, G.; Bikovens, O.; Telysheva, G. Characterization of Softwood and Hardwood Lignoblast Kraft Lignins with Emphasis on Their Antioxidant Activity. *BioResources* **2014**, *9*, 2051–2068.

(12) Jiang, C.; Bo, J.; Xiao, X.; Zhang, S.; Wang, Z.; Yan, G.; Wu, Y.; Wong, C.; He, H. Converting Waste Lignin into Nano-Biochar as a Renewable Substitute of Carbon Black for Reinforcing Styrene-Butadiene Rubber. *Waste Manage.* **2020**, *102*, 732–742.

(13) Alexy, P.; Košíková, B.; Podstránska, G. The Effect of Blending Lignin with Polyethylene and Polypropylene on Physical Properties. *Polymer* **2000**, *41*, 4901–4908.

(14) Mu, L.; Wu, J.; Matsakas, L.; Chen, M.; Rova, U.; Christakopoulos, P.; Zhu, J.; Shi, Y. Two Important Factors of Selecting Lignin as Efficient Lubricating Additives in Poly (Ethylene Glycol): Hydrogen Bond and Molecular Weight. *Int. J. Biol. Macromol.* **2019**, *129*, 564–570.

(15) Hua, J.; Shi, Y. Non-Corrosive Green Lubricant With Dissolved Lignin in Ionic Liquids Behave as Ideal Lubricants for Steel-DLC Applications. *Front. Chem.* **2019**, *7*, No. 755.

(16) Beaucamp, A.; Wang, Y.; Culebras, M.; Collins, M. N. Carbon Fibres from Renewable Resources: The Role of the Lignin Molecular Structure in Its Blendability with Biobased Poly(Ethylene Terephthalate). *Green Chem.* **2019**, *21*, 5063–5072.

(17) Jin, J.; Ogale, A. A. Carbon Fibers Derived from Wet-Spinning of Equi-Component Lignin/Polyacrylonitrile Blends. *J. Appl. Polym. Sci.* **2018**, *135*, No. 45903.

(18) Gao, W.; Fatehi, P. Lignin for Polymer and Nanoparticle Production: Current Status and Challenges. *Can. J. Chem. Eng.* **2019**, *97*, 2827–2842.

(19) Luo, M.; Lin, H.; Li, B.; Dong, Y.; He, Y.; Wang, L. A Novel Modification of Lignin on Corn-cob-Based Biochar to Enhance Removal of Cadmium from Water. *Bioresour. Technol.* **2018**, *259*, 312–318.

(20) Wang, B.; Ran, M.; Fang, G.; Wu, T.; Ni, Y. Biochars from Lignin-Rich Residue of Furfural Manufacturing Process for Heavy Metal Ions Remediation. *Materials* **2020**, *13*, No. 1037.

(21) Riaz, A.; Verma, D.; Zeb, H.; Lee, J. H.; Kim, J. C.; Kwak, S. K.; Kim, J. Solvothermal Liquefaction of Alkali Lignin to Obtain a High Yield of Aromatic Monomers While Suppressing Solvent Consumption. *Green Chem.* **2018**, *20*, 4957–4974.

(22) Kalogiannis, K. G.; Matsakas, L.; Lappas, A. A.; Rova, U.; Christakopoulos, P. Aromatics from Beechwood Organosolv Lignin through Thermal and Catalytic Pyrolysis. *Energies* **2019**, *12*, No. 1606.

(23) Matsakas, L.; Nitsos, C.; Raghavendran, V.; Yakimenko, O.; Persson, G.; Olsson, E.; Rova, U.; Olsson, L.; Christakopoulos, P. A Novel Hybrid Organosolv: Steam Explosion Method for the Efficient Fractionation and Pretreatment of Birch Biomass. *Biotechnol. Biofuels* **2018**, *11*, No. 522.

(24) Aguilera-Segura, S. M.; Bossu, J.; Corn, S.; Trens, P.; Mineva, T.; Le Moigne, N.; Di Renzo, F. Synergistic Sorption of Mixed Solvents in Wood Cell Walls: Experimental and Theoretical Approach. *Macromol. Symp.* **2019**, *386*, No. 1900022.

(25) Wen, J. L.; Xue, B. L.; Sun, S. L.; Sun, R. C. Quantitative Structural Characterization and Thermal Properties of Birch Lignins after Auto-Catalyzed Organosolv Pretreatment and Enzymatic Hydrolysis. *J. Chem. Technol. Biotechnol.* **2013**, *88*, No. 1663.

(26) Zhang, L.; Gellerstedt, G. Quantitative 2D HSQC NMR Determination of Polymer Structures by Selecting Suitable Internal Standard References. *Magn. Reson. Chem.* **2007**, *45*, 37–45.

(27) Belyy, V. A.; Kanmanov, A. P.; Kocheva, L. S.; Nekrasova, P. S.; Kaneva, M. V.; Lobov, A. N.; Spirikhin, L. V. Comparative Study of Chemical and Topological Structure of Macromolecules of Lignins of Birch (*Betula Verrucosa*) and Apple (*Malus Domestica*) Wood. *Int. J. Biol. Macromol.* **2019**, *128*, 40–48.

(28) Zhao, B.; O'Connor, D.; Zhang, J.; Peng, T.; Shen, Z.; Tsang, D. C. W.; Hou, D. Effect of Pyrolysis Temperature, Heating Rate, and Residence Time on Rapeseed Stem Derived Biochar. *J. Cleaner Prod.* **2018**, *174*, 977–987.

(29) Mullen, C. A.; Boateng, A. A. Catalytic Pyrolysis-GC/MS of Lignin from Several Sources. *Fuel Process. Technol.* **2010**, *91*, 1446–1458.

(30) Kim, J. Y.; Oh, S.; Hwang, H.; Kim, U. J.; Choi, J. W. Structural Features and Thermal Degradation Properties of Various Lignin Macromolecules Obtained from Poplar Wood (*Populus Albaglandulosa*). *Polym. Degrad. Stab.* **2013**, *98*, 1671–1678.

(31) Muraliedharan, M. N.; Zouraris, D.; Karantonis, A.; Topakas, E.; Sandgren, M.; Rova, U.; Christakopoulos, P.; Karnaouri, A. Effect of Lignin Fractions Isolated from Different Biomass Sources on Cellulose Oxidation by Fungal Lytic Polysaccharide Monoxygenases. *Biotechnol. Biofuels* **2018**, *11*, 1–15.

(32) Watkins, D.; Nuruddin, M.; Hosur, M.; Tcherbi-Narteh, A.; Jeelani, S. Extraction and Characterization of Lignin from Different Biomass Resources. *J. Mater. Res. Technol.* **2015**, *4*, 26–32.

(33) Liu, C.; Hu, J.; Zhang, H.; Xiao, R. Thermal Conversion of Lignin to Phenols: Relevance between Chemical Structure and Pyrolysis Behaviors. *Fuel* **2016**, *182*, 864–870.

(34) Chen, S.; Cheng, H.; Wu, S. Pyrolysis Characteristics and Volatiles Formation Rule of Organic Solvent Fractionized Kraft Lignin. *Fuel* **2020**, *270*, No. 117520.

(35) Faravelli, T.; Frassoldati, A.; Migliavacca, G.; Ranzi, E. Detailed Kinetic Modeling of the Thermal Degradation of Lignins. *Biomass Bioenergy* **2010**, *34*, 290–301.

(36) Tarasov, D.; Leitch, M.; Fatehi, P. Lignin-Carbohydrate Complexes: Properties, Applications, Analyses, and Methods of Extraction: A Review. *Biotechnol. Biofuels* **2018**, *11*, 269.

(37) Giummarella, N.; Pu, Y.; Ragauskas, A. J.; Lawoko, M. A Critical Review on the Analysis of Lignin Carbohydrate Bonds. *Green Chem.* **2019**, *21*, 1573–1595.

(38) Weidener, D.; Klose, H.; Leitner, W.; Schurr, U.; Usadel, B.; de María, P. D.; Grande, P. M. One-Step Lignocellulose Fractionation by Using 2,5-Furandicarboxylic Acid as a Biogenic and Recyclable Catalyst. *ChemSusChem* **2018**, *11*, 2051–2056.

(39) Yao, L.; Chen, C.; Yoo, C. G.; Meng, X.; Li, M.; Pu, Y.; Ragauskas, A. J.; Dong, C.; Yang, H. Insights of Ethanol Organosolv Pretreatment on Lignin Properties of *Broussonetia Papyrifera*. *ACS Sustainable Chem. Eng.* **2018**, *6*, 14767–14773.

(40) Paszner, L.; Behera, N. C. Topochemistry of Softwood Delignification by Alkali Earth Metal Salt Catalysed Organosolv Pulping. *Holzforchung* **1989**, *43*, 159–168.

(41) Bauer, S.; Sorek, H.; Mitchell, V. D.; Ibáñez, A. B.; Wemmer, D. E. Characterization of *Miscanthus Giganteus* Lignin Isolated by Ethanol Organosolv Process under Reflux Condition. *J. Agric. Food Chem.* **2012**, *60*, No. 8203.

(42) Lancefield, C. S.; Panovic, I.; Deuss, P. J.; Barta, K.; Westwood, N. J. Pre-Treatment of Lignocellulosic Feedstocks Using Biorenewable Alcohols: Towards Complete Biomass Valorisation. *Green Chem.* **2017**, *19*, No. 202.

(43) Zijlstra, D. S.; Lahive, C. W.; Analbers, C. A.; Figueirêdo, M. B.; Wang, Z.; Lancefield, C. S.; Deuss, P. J. Mild Organosolv Lignin Extraction with Alcohols: The Importance of Benzylic Alkoxylation. *ACS Sustainable Chem. Eng.* **2020**, *8*, No. 5119.

(44) Brandt, A.; Chen, L.; Van Dongen, B. E.; Welton, T.; Hallett, J. P. Structural Changes in Lignins Isolated Using an Acidic Ionic Liquid Water Mixture. *Green Chem.* **2015**, *17*, 5019–5034.

(45) Bouxin, F. P.; David Jackson, S.; Jarvis, M. C. Organosolv Pretreatment of Sitka Spruce Wood: Conversion of Hemicelluloses to Ethyl Glycosides. *Bioresour. Technol.* **2014**, *151*, 441–444.

(46) Appeldoorn, M. M.; De Waard, P.; Kabel, M. A.; Gruppen, H.; Schols, H. A. Enzyme Resistant Feruloylated Xylooligomer Analogues from Thermochemically Treated Corn Fiber Contain Large Side Chains, Ethyl Glycosides and Novel Sites of Acetylation. *Carbohydr. Res.* **2013**, *381*, 33–42.

(47) Zhang, J.; Heiss, C.; Thorne, P. G.; Bal, C.; Azadi, P.; Lynd, L. R. Formation of Ethyl β -Xylopyranoside during Simultaneous Saccharification and Co-Fermentation of Paper Sludge. *Enzyme Microb. Technol.* **2009**, *44*, 196–202.

(48) Huijgen, W. J. J.; Telysheva, G.; Arshanitsa, A.; Gosselink, R. J. A.; de Wild, P. J. Characteristics of Wheat Straw Lignins from Ethanol-Based Organosolv Treatment. *Ind. Crops Prod.* **2014**, *59*, 85–95.

(49) Kubo, S.; Kadla, J. F. Poly(Ethylene Oxide)/Organosolv Lignin Blends: Relationship between Thermal Properties, Chemical Structure, and Blend Behavior. *Macromolecules* **2004**, *37*, 6904–6911.

(50) El Hage, R.; Brosse, N.; Sannigrahi, P.; Ragauskas, A. Effects of Process Severity on the Chemical Structure of Miscanthus Ethanol Organosolv Lignin. *Polym. Degrad. Stab.* **2010**, *95*, 997–1003.

(51) Berlin, A.; Balakshin, M. *Industrial Lignins: Analysis, Properties, and Applications*; Elsevier, 2014.

(52) Vermaas, J. V.; Crowley, M. F.; Beckham, G. T. A Quantitative Molecular Atlas for Interactions between Lignin and Cellulose. *ACS Sustainable Chem. Eng.* **2019**, *7*, 19570–19583.

(53) Lange, H.; Rulli, F.; Crestini, C. Gel Permeation Chromatography in Determining Molecular Weights of Lignins: Critical Aspects Revisited for Improved Utility in the Development of Novel Materials. *ACS Sustainable Chem. Eng.* **2016**, *4*, 5167–5180.

(54) Granata, A.; Argyropoulos, D. S. 2-Chloro-4,4,5,5-Tetramethyl-1,3,2-Dioxaphospholane, a Reagent for the Accurate Determination of the Uncondensed and Condensed Phenolic Moieties in Lignins. *J. Agric. Food Chem.* **1995**, *43*, 1538–1544.